MINISTÉRIO DA EDUCAÇÃO
Fundação Universidade Federal da Grande Dourados
Pró-Reitoria de Ensino de Graduação

UFGD
Universidade Federal
da Grande Dourados

TRABALHO DE CONCLUSÃO DE CURSO

DESIGN, CONSTRUCTION, AND TESTING OF A LOW-COST AERODYNAMIC FORCE MEASUREMENT SYSTEM FOR A SUBSONIC WIND TUNNEL

DIONNATAN GABRIEL RETAMERO DA SILVA

Dourados - MS
2025

DIONNATAN GABRIEL RETAMERO DA SILVA

DESIGN, CONSTRUCTION, AND TESTING OF A LOW-COST AERODYNAMIC FORCE MEASUREMENT SYSTEM FOR A SUBSONIC WIND TUNNEL

Trabalho de Conclusão de Curso apresentado ao Curso de Engenharia Mecânica da Universidade Federal da Grande Dourados (UFGD), como requisito parcial para a obtenção do título de Bacharel em Engenharia Mecânica.

Orientador: Prof. Augusto Salomão Bornschlegell

Área de concentração: Mecânica dos Fluidos Experimental

Dourados - MS
2025

MINISTÉRIO DA EDUCAÇÃO
FUNDAÇÃO UNIVERSIDADE FEDERAL DA GRANDE DOURADOS

ANEXO D - AVALIAÇÃO FINAL DO TRABALHO DE CONCLUSÃO DE CURSO

Aluno: **DIONNATAN GABRIEL RETAMERO DA SILVA**

Título do trabalho e subtítulo (se houver): **DESIGN, CONSTRUCTION, AND TESTING OF A LOW-COST AERODYNAMIC FORCE MEASUREMENT SYSTEM FOR A SUBSONIC WIND TUNNEL**

BANCA EXAMINADORA

1. **Presidente (orientador):**
Prof. Dr. Augusto Salomão Bornschlegell, Universidade Federal da Grande Dourados - UFGD

2. **Membro:**
Prof. Dr. Bruno Arantes Moreira, Universidade Federal da Grande Dourados - UFGD

3. **Membro:**
Profa. Dra. Isabele Oliveira de Paula, Universidade Federal da Grande Dourados - UFGD

De acordo com o grau final obtido pelo aluno, nós da banca examinadora, declaramos APROVADO o aluno acima identificado, na componente curricular Trabalho de Conclusão de Curso (TCC-II) de Graduação no Curso de Engenharia Mecânica da Universidade Federal da Grande Dourados.

Dourados, 15 de dezembro de 2025.

gov.br Documento assinado digitalmente
AUGUSTO SALOMAO BORNSCHLEGELL
Data: 17/12/2025 10:40:21-0300
Verifique em https://validar.iti.gov.br

Prof. Dr. Augusto Salomão Bornschlegell

gov.br Documento assinado digitalmente
BRUNO ARANTES MOREIRA
Data: 15/12/2025 17:07:13-0300
Verifique em https://validar.iti.gov.br

Prof. Dr. Bruno Arantes Moreira

gov.br Documento assinado digitalmente
ISABELE OLIVEIRA DE PAULA
Data: 15/12/2025 17:19:09-0300
Verifique em https://validar.iti.gov.br

Profa. Dra. Isabele Oliveira de Paula

RESUMO

Este trabalho apresenta o projeto, construção e avaliação experimental de um sistema de medição de forças aerodinâmicas externas de baixo custo para túneis de vento subsônicos. Visando superar os custos proibitivos da instrumentação comercial na educação em engenharia, o projeto desenvolveu uma solução personalizada priorizando a integridade estrutural e a viabilidade de manutenção. A metodologia construtiva adotou uma arquitetura rígida em aço soldado para minimizar a deflexão mecânica e a histerese, integrada a células de carga do tipo *bending beam* modulares para permitir a escalabilidade dos sensores. A caracterização do sistema compreendeu a calibração estática, que confirmou alta linearidade ($R^2 \approx 1.0$) e *offsets* de zero estáveis, seguida por testes aerodinâmicos utilizando cilindros e um aerofólio NACA 0012. Os resultados estabeleceram um envelope operacional confiável para velocidades de corrente livre superiores a 10 m/s, onde a relação sinal-ruído torna-se ótima. Uma análise comparativa entre cilindros de 25 mm e 100 mm demonstrou o impacto crítico do confinamento da parede: o modelo maior exibiu coeficientes de arrasto superestimados devido a uma razão de bloqueio de 21,6%, enquanto o corpo de prova de 25 mm produziu resultados consistentes com a literatura subcrítica ($C_D \approx 1.18$). Além disso, o sistema resolveu com sucesso os efeitos de asa finita no aerofólio, capturando a penalidade de arrasto induzido. Conclui-se que a arquitetura proposta fornece uma plataforma robusta e modular para pesquisa educacional e aplicada, desde que respeitadas as condições de contorno geométricas.

Palavras-chave: Túnel de vento. Balança aerodinâmica. Baixo custo. Instrumentação. Efeitos de bloqueio.

ABSTRACT

This work presents the design, construction, and experimental assessment of a low-cost external aerodynamic force measurement system for a subsonic wind tunnel. Aiming to overcome the prohibitive costs of commercial instrumentation in engineering education, the project developed a customized solution prioritizing structural integrity and maintenance feasibility. The construction methodology adopted a rigid welded steel architecture to minimize mechanical deflection and hysteresis, integrated with modular bending beam load cells to allow for sensor scalability. The system characterization comprised static calibration, which confirmed high linearity ($R^2 \approx 1.0$) and stable zero offsets, followed by aerodynamic testing using cylinders and a NACA 0012 airfoil. Results established a reliable operational envelope for freestream velocities exceeding 10 m/s, where the signal-to-noise ratio becomes optimal. A comparative analysis between 25 mm and 100 mm cylinders demonstrated the critical impact of wall confinement: the larger model exhibited overestimated drag coefficients due to a 21.6% blockage ratio, while the 25 mm specimen yielded results consistent with subcritical literature ($C_D \approx 1.18$). Furthermore, the system successfully resolved finite wing effects on the airfoil, capturing the induced drag penalty. It is concluded that the proposed architecture provides a robust, modular platform for educational and applied research, provided that geometric boundary conditions are respected.

Keywords: Wind tunnel. Aerodynamic balance. Low-cost. Instrumentation. Blockage effects.

ENCIT2026
21st Brazilian Congress of Thermal Sciences and Engineering

ABCM
Associação Brasileira de Engenharia e Ciências Mecânicas

21th Brazilian Congress of Thermal Sciences and Engineering
November 08th–12th, 2026, Santos - SP - Brazil

ENC-2026-XXXX
DESIGN, CONSTRUCTION, AND TESTING OF A LOW-COST AERODYNAMIC FORCE MEASUREMENT SYSTEM FOR A SUBSONIC WIND TUNNEL

Dionnatan Gabriel Retamero da Silva
dionnatan.silva060@academico.ufgd.edu.br
Augusto Salomão Bornschlegell
augustosalomao@ufgd.edu.br
Universidade Federal da Grande Dourados, Faculdade de Engenharia, Dourados, Mato Grosso do Sul, Brasil.

Abstract. *This work presents the design, construction, and experimental assessment of a low-cost external aerodynamic force measurement system for a subsonic wind tunnel. Aiming to overcome the prohibitive costs of commercial instrumentation in engineering education, the project developed a customized solution prioritizing structural integrity and maintenance feasibility. The construction methodology adopted a rigid welded steel architecture to minimize mechanical deflection and hysteresis, integrated with modular bending beam load cells to allow for sensor scalability. The system characterization comprised static calibration, which confirmed high linearity ($R^2 \approx 1.0$) and stable zero offsets, followed by aerodynamic testing using cylinders and a NACA 0012 airfoil. Results established a reliable operational envelope for freestream velocities exceeding 10 m/s, where the signal-to-noise ratio becomes optimal. A comparative analysis between 25 mm and 100 mm cylinders demonstrated the critical impact of wall confinement: the larger model exhibited overestimated drag coefficients due to a 21.6% blockage ratio, while the 25 mm specimen yielded results consistent with subcritical literature ($C_D \approx 1.18$). Furthermore, the system successfully resolved finite wing effects on the airfoil, capturing the induced drag penalty. It is concluded that the proposed architecture provides a robust, modular platform for educational and applied research, provided that geometric boundary conditions are respected.*
Keywords: *External Balance, Subsonic Wind Tunnel, Low-Cost Instrumentation, Blockage Ratio, Aerodynamic Testing.*

1. INTRODUCTION

Experimental validation of fluid mechanics theories is a fundamental stage in engineering education. The wind tunnel is a primary tool in this process, enabling the simulation of flows around test bodies. However, the acquisition and maintenance costs of commercial aerodynamic data acquisition systems often exceed the budget of educational institutions. This constraint limits the scope of practical classes and extension projects. Consequently, the development of a low-cost measurement system presents a solution to enable the quantitative measurement of lift and drag forces on scaled models.

The state of the art in aerodynamic instrumentation presents various solutions depending on the flow regime and required precision. Advanced works, such as those by Boutemedjet *et al.* (2018) and Sun *et al.* (2024), demonstrate the application of internal balances installed within the test model. Although these configurations reduce aerodynamic interference in transonic and hypersonic regimes, they impose geometric constraints, as each model requires an adapted balance or specific internal volume. Additionally, the calibration of these devices often demands complex algorithms to compensate for non-linear couplings, as proposed by Yingkun *et al.* (2013). For an institution implementing its first operational system, the adoption of such architectures is incompatible with the current infrastructure.

Given the manufacturing constraints, the literature identifies external balances as a viable alternative for subsonic wind tunnels. Julian *et al.* (2024) numerically validate this approach, indicating that external systems offer adequate precision for low Reynolds numbers. However, the constructive simplicity of the external balance involves the challenge of structural rigidity. Saleh and Ravkoolpour (2016) notes that external transmission systems are subject to uncertainties generated by mechanical deformations. The author states that project results depend on the definition of geometry and material to mitigate hysteresis, a point also addressed in the structural optimizations of Hanapur *et al.* (2022).

This analysis guided the design philosophy of the present work. While additive manufacturing is a valid method for prototyping, preliminary evaluations indicated that achieving the necessary structural stiffness with polymeric materials would require extensive optimization of printing parameters. To ensure operational reliability within the available resources, the design strategy prioritized a deterministic solution. Consequently, the project utilized an external system based on a welded steel architecture.

In this scenario of technical convergence and institutional demands, the primary objective of this study is the design, construction, and characterization of a low-cost aerodynamic force measurement system. The approach adopts an incremental design philosophy wherein functional robustness and sensor modularity precede complexity. The proposed

solution consists of a rigid external balance equipped with interchangeable commercial load cells. The instrument's performance is assessed through statistical treatment of experimental data and by comparing the drag and lift coefficients obtained in cylinder and airfoil tests against classic literature curves and published experimental data.

2. METHODOLOGY

2.1 Experimental Setup and Structural Design

The experimental tests were conducted in an open-circuit subsonic wind tunnel (Model AA-TVSH1/H1, Aeroalcool). The apparatus features a test section with dimensions of $462 \times 462 \times 1200$ mm. The freestream velocity is continuously adjustable, reaching a maximum limit of 25 m/s. The general configuration of the wind tunnel is presented in Fig. 1.

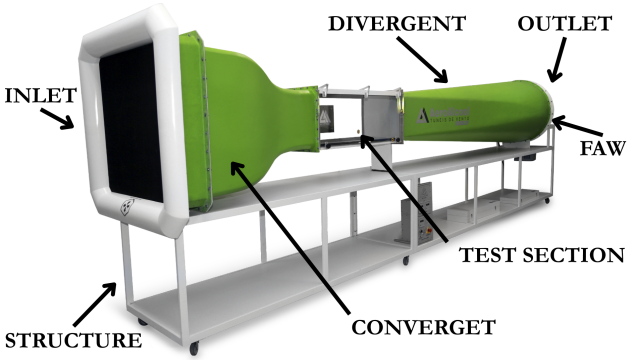

Figure 1: Isometric view of the AA-TVSH1 wind tunnel.

The measurement system was designed as an external balance mounted on an independent support structure adjacent to the test section. This configuration ensures mechanical isolation from the tunnel vibrations. The structural design employs a welded steel architecture to minimize deflection under load. The working principle relies on the vector decomposition of aerodynamic forces through a serial mechanical arrangement, shown in Fig. 2.

The mechanical chain operates as follows: the Lift load cell acts as the primary support, fixed to the static base in a cantilever configuration. An L-shaped steel bracket connects the free end of the lift sensor to the base of the Drag load cell. Consequently, the Drag sensor supports the model strut. This arrangement ensures that vertical (lift) and horizontal (drag) forces are transmitted to their respective transducers without mechanical locking. The assembly utilizes standardized mounting holes to ensure modularity, allowing for the replacement of load cells or the adjustment of force capacity without structural modifications.

The complete experimental configuration is detailed in Fig. 2. The internal view (Fig. 2a) displays the test specimen (NACA 0012 airfoil) positioned within the test section, highlighting the visual protractor used for angle of attack control. The external view (Fig. 2b) presents the balance assembly with the critical mechanical components identified.

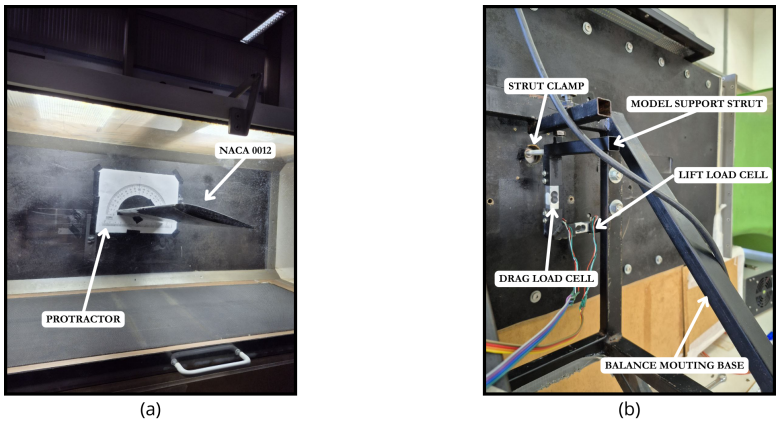

(a) (b)

Figure 2: Experimental setup visualization: (a) Internal view of the test section with the NACA 0012 airfoil and angular control; (b) External view of the measurement system with key components indicated.

2.2 Instrumentation and Sensor Sizing

The instrumentation strategy employed commercial sensors to ensure data reliability and facilitate maintenance. Unlike custom-machined strain gauge elements, commercial bending beam load cells offer standardized calibration parameters and interchangeability.

The sizing process relied on the definitions of the aerodynamic coefficients for drag (C_D) and lift (C_L), as expressed in Eqs. (1) and (2), respectively:

$$C_D = \frac{2F_D}{\rho V^2 A} \tag{1}$$

$$C_L = \frac{2F_L}{\rho V^2 S} \tag{2}$$

where F_D and F_L are the aerodynamic forces, ρ is the air density, V is the freestream velocity, and A and S correspond to the reference areas. To select the nominal capacity, these relations were solved for force (F) to estimate the maximum loads expected at the tunnel's top speed (25 m/s), considering a flat plate ($C_D \approx 2.0$) and a NACA 0012 airfoil at stall ($C_{L,max} \approx 1.5$) as critical loading conditions.

A comparative analysis indicated that 1 kg and 3 kg units would risk saturation under these limit conditions. Consequently, 5 kg load cells were selected for this initial experimental assessment. The adequacy of this capacity is corroborated by the response curves in Fig. 3. Fig. 3a shows that the drag demand remains within the linear operating zone (green area). Concurrently, Fig. 3b demonstrates that the system's tare weight consumes a fraction of the sensor's range, preserving dynamic margin for lift measurement. It is noted that the system's modular design allows for the future installation of lower capacity sensors (e.g., 1 kg) to increase resolution for experiments at lower velocities, provided that overload limits are respected.

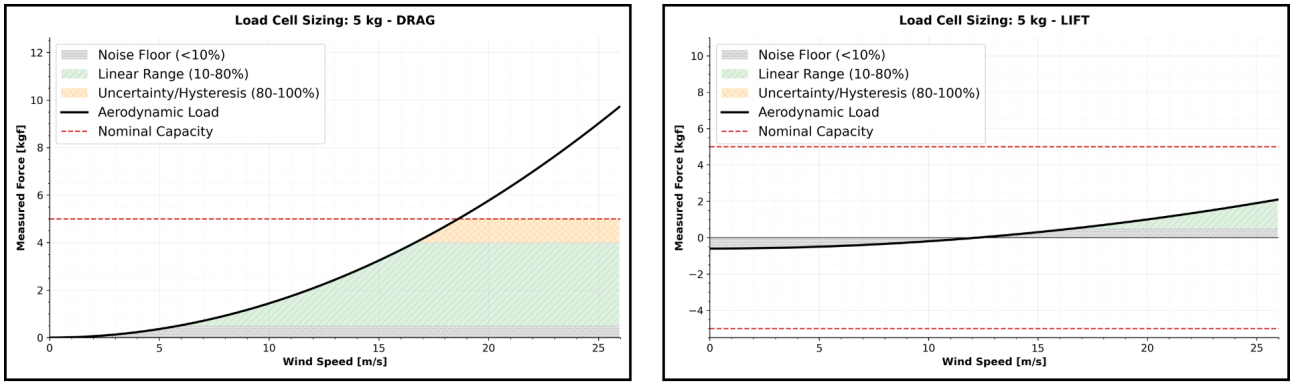

(a) (b)

Figure 3: Load cell sizing analysis for 5 kg capacity: (a) Lift capacity analysis demonstrating margin above the system tare; (b) Aerodynamic drag demand curve (black) relative to the linear operating zone (green).

The data acquisition architecture employs an ATmega328P microcontroller (Arduino Uno), interfaced with 24-bit HX711 analog-to-digital converter modules. A micro SD card module was integrated for local data logging. To avoid processing latency during testing, the system records raw digital signals, which are converted into force units during the post-processing stage. The complete hardware assembly is detailed in the experimental calibration setup presented in the subsequent section (see Fig. 4a).

2.3 Calibration Procedure and Uncertainty Analysis

The metrological characterization of the measurement system was conducted through a static calibration procedure involving the sequential application of gravitational loads. The reference forces were generated using discrete masses, individually quantified using a digital precision scale to ensure value accuracy. This method covered the operational range of the sensors, with a total of 12 load steps recorded for each channel. The experimental arrangement is illustrated in Fig. 4, detailing the data acquisition hardware (Fig. 4a) and the physical calibration rig (Fig. 4b).

Data processing was performed using the Python 3.12 language. In contrast to the Ordinary Least Squares (OLS) method, this study employed Orthogonal Distance Regression (ODR) to account for uncertainties associated with both the dependent variable (sensor reading) and the independent variable (applied mass measurement). The regression analysis was executed using the `scipy.odr` module from the SciPy library. Concurrently, the uncertainty propagation was computed via direct vector implementation of the ISO GUM (2008) equations using the NumPy library.

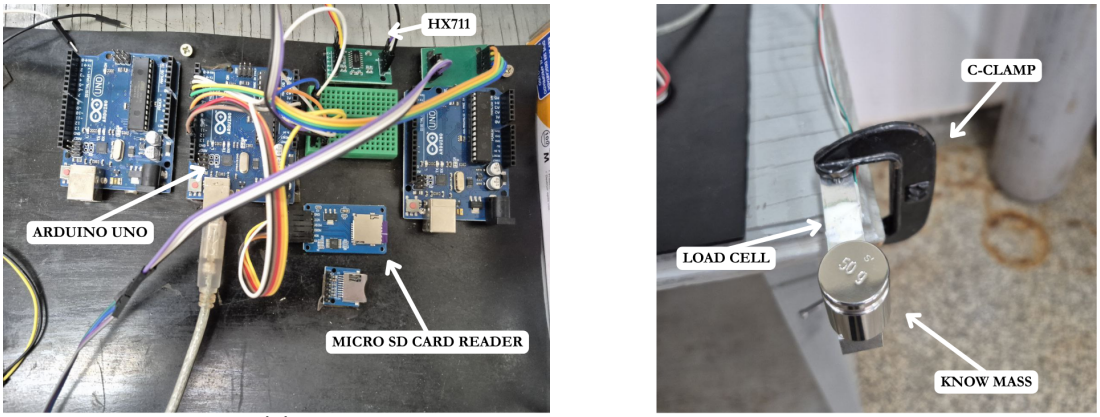

(a) (b)

Figure 4: Experimental calibration setup: (a) Data acquisition hardware assembly; (b) Static calibration arrangement using gravitational loading.

The system transfer function follows the linear model expressed in Eq. (3), where F_{cal} corresponds to the calibrated force and S_{dig} to the discretized digital signal. The sensitivity coefficients (α) and the offset term (β) were determined statistically to minimize orthogonal residuals.

$$F_{cal} = \alpha \cdot S_{dig} + \beta \tag{3}$$

Measurement uncertainty quantification adhered to the guidelines stipulated by the Guide to the Expression of Uncertainty in Measurement (ISO GUM). For each load step, the Type A standard uncertainty was derived from the statistical dispersion of samples (n). The expanded uncertainty (U) was obtained by applying a coverage factor $k = 2$, providing a confidence level of approximately 95% to the results.

2.4 Test Specimens and Experimental Protocol

Given the finite dimensions of the wind tunnel test section ($H = 462$ mm), the Blockage Ratio (BR) constitutes a critical parameter for data validity. Defined as the ratio between the model's frontal dimension (d) and the tunnel's cross-sectional height (H), the BR is calculated as:

$$BR = \frac{d}{H} \tag{4}$$

This parameter quantifies the flow restriction caused by the model's presence. As detailed by Mondal and Alam (2023), wall confinement accelerates the local flow around the body due to mass conservation (Venturi effect), artificially increasing the measured drag forces compared to free-stream conditions. According to the criteria established by Mondal and Alam (2023), blockage effects are considered negligible for $BR \leq 6\%$. Based on these boundary conditions, the experimental protocol utilized three test specimens, standardized with an effective span of 455 mm:

- **Cylinder A (100 mm):** Constructed from painted PVC. It is characterized by a blockage ratio of $BR \approx 21.6\%$, representing a confined flow condition to evaluate wall interference effects.

- **Cylinder B (25 mm):** Constructed from painted PVC. With a blockage ratio of $BR \approx 5.4\%$, it is situated within the range of minimal wall interference, serving as the control case for subcritical flow.

- **NACA 0012 Airfoil:** A smooth-surface fiberglass wing with a chord length of 250 mm. This model was selected to validate the system's ability to resolve aerodynamic polars and finite wing effects.

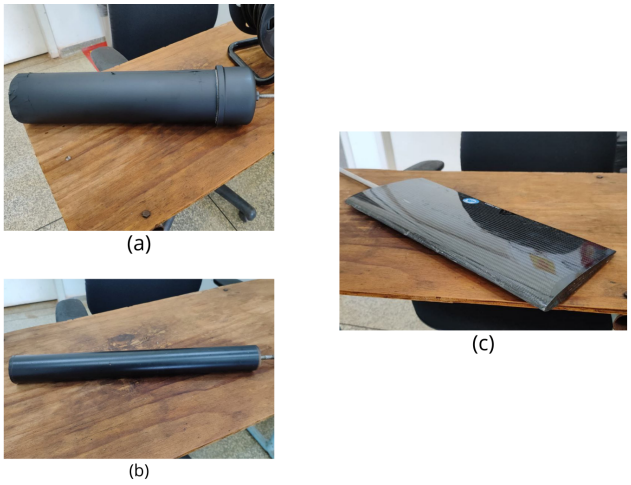

Figure 5: Test specimens used in the experimental testing: (a) 100 mm Cylinder ($BR \approx 21.6\%$); (b) 25 mm Cylinder ($BR \approx 5.4\%$); (c) NACA 0012 Airfoil (chord = 250 mm).

The experimental protocol included environmental compensation for the calculation of aerodynamic coefficients. Air density (ρ) was determined analytically for each data point based on instantaneous readings of local atmospheric pressure (P_{atm}) and temperature (T), using the ideal gas equation:

$$\rho = \frac{P_{atm}}{R_{air} \cdot T} \tag{5}$$

where R_{air} is the specific gas constant for dry air.

For the NACA 0012 airfoil, a baseline correction was applied based on its geometric symmetry, which dictates zero lift at zero angle of attack ($\alpha = 0°$). The residual lift measured at this condition was treated as a systematic offset and subtracted from the entire dataset. This correction compensates for static deviations regarding initial alignment tolerances.

The testing protocol consisted of varying the freestream velocity in discrete increments, reaching a maximum of 25 m/s. The airfoil was tested at discrete angles of attack to verify the measurement of lift and induced drag components. For each velocity step, continuous data logging was performed. The time history of the raw electrical signals, exemplified in Fig. 6 for $\alpha = 5°$, was analyzed to identify the flow stabilization period and define the valid sampling window for calculating the mean force values and experimental uncertainty.

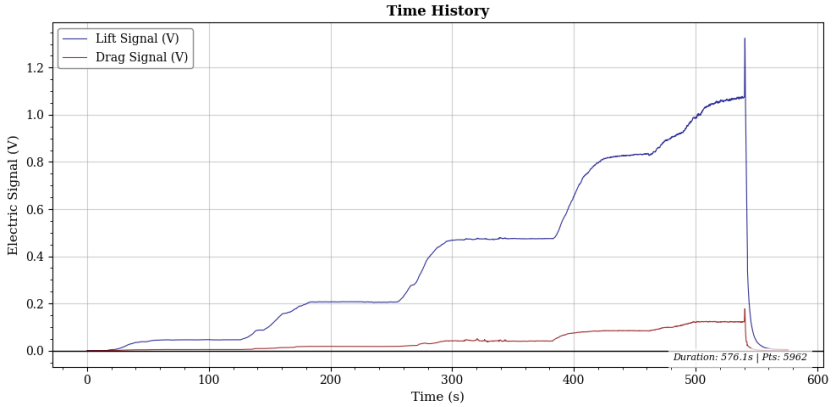

Figure 6: Time history of raw electrical signals recorded at 25 m/s freestream velocity and $\alpha = 5°$: Curve 01 (Drag) and Curve 02 (Lift).

3. Results and Discussion

3.1 Metrological Characterization: Calibration Curves

The reliability of the experimental data depends on the metrological characterization of the measurement system. Following the static calibration procedure described in the methodology, the linear relationship between the applied gravitational loads and the transducers' electrical response was established. Figure 7 presents the calibration curves for both the Lift and Drag channels.

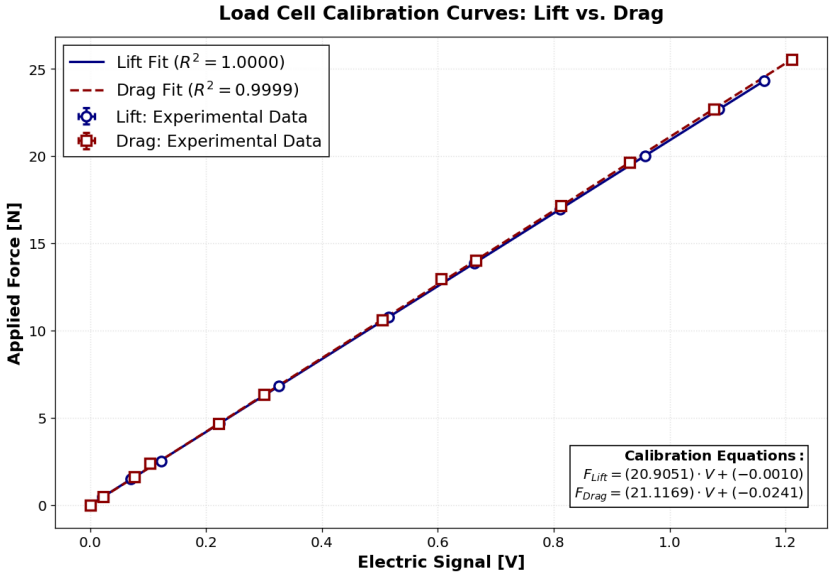

Figure 7: Static calibration curves for lift and drag channels, showing the linear transfer functions and coefficients of determination (R^2).

The results indicate linear behavior for both transducers throughout the operational range, yielding coefficients of determination approaching unity ($R^2 \approx 1.0$). Furthermore, stable zero offsets were observed during the tests. These characteristics are essential for ensuring measurement precision in low Reynolds number flows. The obtained transfer functions enable the conversion of digital signals into force units, confirming the system's suitability for aerodynamic data acquisition.

4. Cylinder Aerodynamic Characterization and Blockage Analysis

The accuracy of the measurement system was assessed by comparing the experimental drag coefficients (C_D) of the 25 mm and 100 mm cylinders against established literature ranges. To ensure a quantitative comparison, data points from reference authors were extracted from published plots using digital image digitization techniques. Figure 8 presents the drag coefficient evolution as a function of the Reynolds number (Re).

The experimental protocol employed discrete velocity increments to map the Reynolds number dependence. While the current campaign focused on validating the ability of the system to capture critical aerodynamic trends, specifically drag stabilization and blockage effects, the modular control architecture supports finer velocity discretization for future investigations.

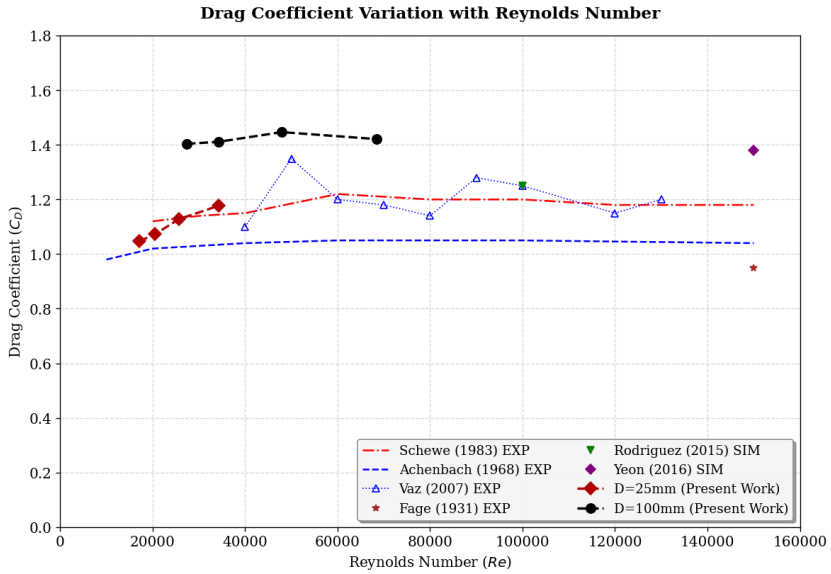

Figure 8: Comparison of experimental drag coefficients for 25 mm and 100 mm cylinders against literature baselines.

For the 25 mm cylinder ($BR \approx 5.4\%$), the analysis was restricted to the operational range where the aerodynamic signal exceeds the noise floor of the sensor ($Re > 1.5 \times 10^4$). In this reliable interval, the data converges to a mean value of $C_D \approx 1.18$. It is important to distinguish the experimental conditions from theoretical ideals. While the canonical value of $C_D \approx 1.2$ refers to smooth infinite cylinders, the test specimen is a finite cylinder constructed from painted PVC. Experimental literature reports a scatter of subcritical drag coefficients ($1.0 \leq C_D \leq 1.3$) depending on surface roughness and aspect ratio. In this context, the obtained result (1.18) is consistent with data from Schewe (1983) and lies within the expected range for finite cylinders ($L/D \approx 18$), similar to the low blockage experiments ($BR < 6\%$) conducted by Vaz (2007).

Conversely, the 100 mm cylinder ($BR \approx 21.6\%$) exhibits a stabilized drag coefficient of $C_D \approx 1.45$. Even considering natural data dispersion, this magnitude exceeds the upper bound of the subcritical regime. This behavior aligns with the findings of **?**, who reported that experiments with $BR \geq 20\%$ consistently result in overestimated drag coefficients due to flow acceleration or the Venturi effect. Consequently, this elevated C_D is identified as a physical manifestation of severe wall confinement.

It is noteworthy that testing for the 100 mm cylinder was terminated at $Re \approx 7.0 \times 10^4$ ($V \approx 10$ m/s). Beyond this threshold, the model exhibited aeroelastic instability characterized by static deflection and oscillation. To preserve the structural integrity of the wind tunnel test section and the measurement equipment, the protocol was restricted to this safety limit.

5. Characterization of the NACA 0012 Airfoil

The aerodynamic performance of the NACA 0012 airfoil was evaluated to verify the ability of the measurement system to resolve lift (C_L) and drag (C_D) components. The analysis focuses on identifying the discrepancies between the experimental data obtained for a finite wing and the theoretical predictions for infinite or 2D profiles. Since the blockage ratio for the airfoil is significantly lower than that of the large cylinder, the discussion prioritizes finite wing effects as the dominant source of deviation from 2D theory.

5.1 Lift Coefficient and Finite Wing Effects

Figure 9 presents the lift curve slope ($C_{L\alpha}$) for Reynolds numbers ranging from 1.7×10^5 to 4.2×10^5. The experimental data exhibits linear behavior up to $\alpha = 10°$ yet with a slope significantly lower than the theoretical 2D value (2π rad^{-1}). The maximum observed C_L is approximately 0.55 at $\alpha = 10°$ whereas 2D data compiled by Sheldahl and Klimas (1981) predicts values near 1.0 for this incidence.

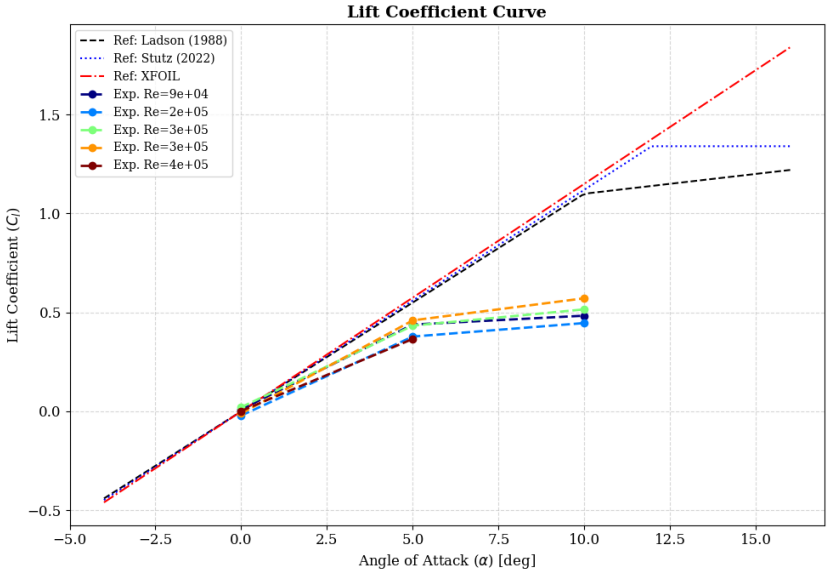

Figure 9: Lift coefficient (C_L) vs. Angle of Attack (α) for different Reynolds numbers, illustrating the finite wing slope reduction.

This attenuation is physically consistent with the finite wing theory described by Anderson (2017). According to this fundamental definition, the pressure differential between the lower and upper surfaces of a finite span wing drives a spanwise flow component that creates wingtip vortices. Anderson (2017) explains that these vortices induce a downward velocity component known as downwash, which effectively reduces the local angle of attack seen by the airfoil sections. Furthermore, the necessary clearance gaps of approximately 7 mm between the model and the tunnel walls allow for

pressure equalization which prevents the establishment of ideal 2D flow. Therefore, the reduced slope confirms that the system is correctly capturing the three dimensional physics inherent to the experimental setup.

5.2 Drag Polar Analysis

The resistive force characteristics are shown in the drag polar (Figure 10). The experimental curve displays a clear parabolic profile distinct from the typical 2D drag curve.

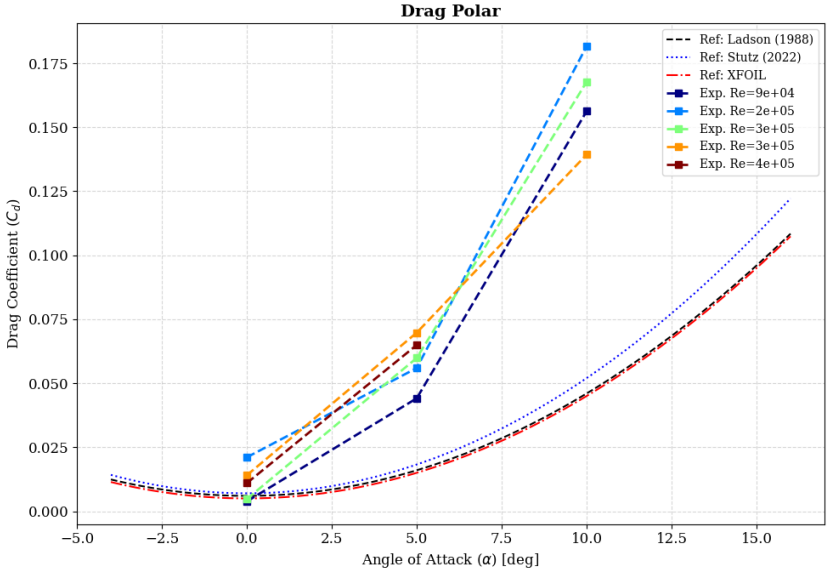

Figure 10: Drag polar (C_D vs. α): Comparison between experimental finite wing data and theoretical 2D profile.

The analysis reveals two primary components contributing to the measured drag. First, the minimum drag at zero lift exceeds the theoretical 2D reference provided by Sheldahl and Klimas (1981). This offset is attributed to interference drag which represents the resistance generated by the interaction between the airflow, the support strut and the wall gaps.

Second, the drag coefficient increases quadratically with lift. This behavior is identified by Anderson (2017) as induced drag (C_{Di}), a component exclusive to finite wings caused by energy dissipation in the trailing vortices. The measurement system successfully resolved this parabolic relationship ($C_D \propto C_L^2$), validating its sensitivity to the aerodynamic phenomena predicted by classical theory for finite aspect ratio wings.

6. CONCLUSIONS

The design, construction, and testing of the external measurement system confirmed the viability of bending beam load cells for subsonic wind tunnel applications. The project validated the incremental design approach, prioritizing structural rigidity and maintenance feasibility.

The welded steel architecture minimized static deflection, while static calibration demonstrated linearity ($R^2 \approx 1.0$) and stable zero offsets. The modular mounting interface allows for sensor interchangeability to accommodate varying load ranges.

Experimental testing defined the operational envelope. Steady-state data reliability is established for freestream velocities above 10 m/s; below this threshold, the signal-to-noise ratio decreases due to sensor resolution limits. Blockage Ratio (BR) analysis confirmed that the 25 mm cylinder ($BR \approx 5.4\%$) yields drag coefficients ($C_D \approx 1.18$) consistent with subcritical literature, whereas the 100 mm cylinder ($BR \approx 21.6\%$) produces overestimated values ($C_D \approx 1.45$) due to wall confinement. Testing of the larger model was terminated at 10 m/s due to observed aeroelastic instability.

Regarding the NACA 0012 airfoil, the system resolved three-dimensional aerodynamic effects, capturing the induced drag penalty and the reduced lift curve slope characteristic of finite wings. Minimum drag offsets were attributed to strut interference and wall gaps.

In conclusion, the system provides a functional platform for aerodynamic investigation. Future work should implement continuous angular sweep algorithms and adapt the support interface for complex geometries, such as suspended vehicular prototypes, ensuring alignment with the overhead balance architecture.

7. REFERENCES

Anderson, J.D., 2017. *Fundamentals of Aerodynamics*. McGraw-Hill Education, New York, NY, 6th edition.

Boutemedjet, A. *et al.*, 2018. "Numerical investigation of the effect of the bucket arc angle on the performance of a savonius wind rotor". *Journal of Renewable and Sustainable Energy*, Vol. 10.

Hanapur, I., Manjunath, S., Hiremath, N., Banapurmath, V., Sajjan, S., Yaliwala, P. and Ayachit, N., 2022. "Improvising the mathematics for effective wind tunnel balance calibration". *Measurement: Sensors*, Vol. 24, p. 100469.

Julian, J., Tjahjana, D., Santoso, W., Hadi, S., Nugraha, A. and Hadi, S., 2024. "Wind tunnel assessment of flow uniformity". *International Journal of Numerical Methods for Heat & Fluid Flow*.

Mondal, R. and Alam, M., 2023. "Blockage effect on wake characteristics of a circular cylinder". *Ocean Engineering*.

Saleh, A. and Ravkoolpour, S., 2016. "Review of tared wind tunnel support interference". *Journal of Aeronautics & Aerospace Engineering*.

Sheldahl, R.E. and Klimas, P.C., 1981. "Aerodynamic characteristics of seven symmetrical airfoil sections through 180-degree angle of attack for use in aerodynamic analysis of vertical axis wind turbines". Technical Report SAND80-2114, Sandia National Laboratories, Albuquerque, NM.

Sun, S. *et al.*, 2024. "Short-time aerodynamic wind tunnel test method". *Ocean Engineering*.

Vaz, G., 2007. "Experimental investigation of the flow around a finite cylinder". *Experiments in Fluids*.

Yingkun, M., Shilin, X., Xinong, Z. and Yajun, L., 2013. "Hybrid calibration method for six-component force/torque transducers of wind tunnel balance based on support vector machines". *Chinese Journal of Aeronautics*, Vol. 26, No. 3, pp. 554–562.

8. Responsibility Notice

The authors are solely responsible for the printed material included in this paper.